**PAPER**

# Pressure dependence of transverse acoustic phonon energy in ferropericlase across the spin transition

View the article online for updates and enhancements.

# Pressure dependence of transverse acoustic phonon energy in ferropericlase across the spin transition

**Hiroshi Fukui**[1,2]**, Alfred Q R Baron**[2]**, Daisuke Ishikawa**[2,3]**,**
**Hiroshi Uchiyama**[2,3]**, Yasuo Ohishi**[3]**, Taku Tsuchiya**[4]**, Hisao Kobayashi**[1]**,**
**Takuya Matsuzaki**[5,6]**, Takashi Yoshino**[5,7] **and Tomoo Katsura**[5,8]

[1] Center for Novel Material Science under Multi-Extreme Conditions, Graduate School of Material Science, University of Hyogo, 3-2-1 Kouto, Kamigori, Hyogo 678–1297, Japan
[2] Materials Dynamics Laboratory, RIKEN SPring-8 Center, 1-1-1 Kouto, Sayo, Hyogo 679-5148, Japan
[3] Research and Utilization Division, Japan Synchrotron Radiation Research Institute (JASRI), SPring-8, 1-1-1 Kouto, Sayo, Hyogo 679-5198, Japan
[4] Geodynamics Research Center, Ehime University, 2-5 Bunkyo-cho, Matsuyama, Ehime 790-8577, Japan
[5] Institute for Study of the Earth's Interior, Okayama University, 827 Yamada, Misasa, Tottori 682-0193, Japan
[6] Present Address: Center for Advanced Marine Core Research, Kochi University, 200 Otsu, Monobe, Nankoku, Kochi 783-8502, Japan
[7] Present Address: Institute for Planetary Materials, Okayama University, 827 Yamada, Misasa, Tottori 682-0193, Japan
[8] Present Address: Bayerisches Geoinstitut, University of Bayreuth, 95440 Bayreuth, Germany

E-mail: fukuih@sci.u-hyogo.ac.jp

CrossMark

## Abstract

We investigated transverse acoustic (TA) phonons in iron-bearing magnesium oxide (ferropericlase) up to 56 GPa using inelastic x-ray scattering (IXS). The results show that the energy of the TA phonon far from the Brillouin zone center suddenly increases with increasing pressure above the spin transition pressure of ferropericlase. *Ab initio* calculations revealed that the TA phonon energy far from the Brillouin zone center is higher in the low-spin state than in the high spin state; that the TA phonon energy depend weakly on pressure; and that the energy gap between the TA and the lowest-energy-optic phonons is much narrower in the low-spin state than in the high-spin state. This allows us to conclude that the anomalous behavior of the TA mode in the present experiments is the result of gap narrowing due to the spin transition and explains contradictory results in previous experimental studies.

Keywords: high pressure, spin transition, inelastic x-ray scattering, *ab initio* calculation, ferropericlase, phonon

(Some figures may appear in colour only in the online journal)

## 1. Introduction

Spin states of transition metals change by applied pressure in some materials. The spin transition under high pressure is accompanied with a sudden volume change because the atomic (ionic) radius of the transition metal depends on the spin state.

The volume change influences elastic properties in the material. Iron-bearing magnesium oxide $Mg_{1-x}Fe_xO$ (ferropericlase) [1] is one example of a material that shows an elastic anomaly [2–6] related to a spin cross-over transition. This material has the NaCl (or B1 in Strukturbericht designation) structure where some of magnesium is substituted by iron.

Previous experimental work showed some results of single crystal elasticity for ferropericlase that are, at first glance, apparently contradictory. Impulsive stimulated light scattering (ISS) [7] showed softenings in three elastic constants ($C_{11}$, $C_{44}$, and $C_{12}$) around the spin transition [2]. Meanwhile, an Inetastic x-ray scattering (IXS) [8] suggested that only $C_{44}$ softens [4]. In addition, a recent study using light scattering techniques (ISS and Brillouin light scattering in which a green laser was used as a probe) reported that $C_{11}$ and $C_{12}$ show softening but $C_{44}$ does not [6].

These results were discussed using calculations of phonon properties based on the planewave-pseudopotential density functional calculations using the local density approximation with the on-site repulsion parameter $U$ (LDA + $U$) [9, 10]. The contradiction described in the foregoing paragraph was attributed to the frequency dependence of pressure derivative of the low-spin fraction of the iron atoms, $n$, in ferropericlase at constant entropy, $\left(\frac{\partial n}{\partial P}\right)_S$. If the volume of ferropericlase, $V$, is expressed as a simple mixture of high- and low-spin ferropericlase, $V_{HS}$ and $V_{LS}$, as $V = (1 - n)V_{HS} + nV_{LS}$, the expression of bulk modulus, which is related to $C_{11}$ and $C_{12}$, contains $\left(\frac{\partial n}{\partial P}\right)_S$ (See equation (6) in [9]). Since $\left(\frac{\partial n}{\partial P}\right)_S$ has a non-zero value, a softening is observed in a longitudinal-wave or bulk-sound velocity. When the lattice-vibration frequency is low, or the period of lattice vibration is longer than the lattice relaxation time after the spin transition, $\left(\frac{\partial n}{\partial P}\right)_S$ will not be negligible [9]. In contrast, $\left(\frac{\partial n}{\partial P}\right)_S$ will be negligible in the higher-frequency lattice vibration, because the lattice relaxation after the spin transition does not occur [9]. Light scattering techniques probe GHz frequencies whereas IXS probes THz frequencies. Therefore, the light scattering techniques showed softening in $C_{11}$ and $C_{12}$ [2, 6] but IXS did not [4]. However, the difference in $\left(\frac{\partial n}{\partial P}\right)_S$ cannot explain why the IXS study [4] showed softening of only $C_{44}$.

A different calculation [9] suggested an alternative origin of the $C_{44}$ anomaly observed using IXS [4]. This study [9] reported an unusual behavior of transverse acoustic (TA) phonon propagating in the [$q00$] direction far from the Brillouin zone center in the high-spin state as pressure is increased. The energy of the [$q00$] TA phonon is related to $C_{44}$ about which the light scattering techniques [2, 6] and IXS [4] showed the contradictory results. The light scattering techniques provide phonon energies very close to the Brillouin zone center, $\Gamma$, point (a corresponding phonon momentum, **q**, is ~0.01 nm$^{-1}$) but cannot measure phonons away from the Brillouin zone center. In contrast, IXS measures phonons away from the zone center, but has difficulty accessing phonons at $\Gamma$, due to strong elastic intensity and its limited momentum resolution (>0.1 nm$^{-1}$). The $q$ values for IXS measurements in [4] were between 1 and 5 nm$^{-1}$. Therefore, a TA phonon anomaly far from the Brillouin zone center might influence the phonons observed by IXS more than those by ISS. We have performed IXS measurements at ambient and high-pressure conditions to shed the light on change in elasticity of

ferropericlase with pressure. *Ab initio* calculations were also performed to interpret the experimental results.

## 2. Experimental methods

Single-crystal samples were synthesized by diffusion of Fe into MgO single crystals from (Mg,Fe)O powder, similar to the method of Jacobsen *et al* [11]. The single crystals of MgO were purchased from Tateho Chemical Industries Co. Ltd, and was cut to $1 \times 1 \times 1$ mm$^3$. (Mg,Fe)O powder was prepared as follows. Sponge iron and magnesium ribbon were solved into dilute nitric acid in Mg:Fe molar ratio of 3:1. Evaporation residue of the nitric acid solution was first kept at a temperature of 400 °C in the atmosphere for a few days, and then at 1245 °C with controlling the oxygen partial pressure close to the iron-wüstite buffer for several hours. The black-color product, $Mg_{0.75}Fe_{0.25}O$, was ground to powder. Several MgO single crystals were embedded into a pellet made of the $Mg_{0.75}Fe_{0.25}O$ powder. The pellet was kept at 1570 °C and an oxygen partial pressure near the iron-wüstite buffer for 150 h, and was then quenched into water.

The symmetry and crystallinity of the synthesized crystals were confirmed by x-ray precession photography. Electron microprobe analysis on the cross section of one of the crystals revealed homogeneous chemical composition. The value of Fe/(Mg + Fe) was $0.161 \pm 0.0087$. Mössbauer spectroscopy with $^{57}$Co source showed $Fe^{3+}/\sum Fe = 0.120$. The results of these composition analyses indicate that the chemical formula of the samples was $Mg_{0.8310}Fe^{2+}_{0.1403}Fe^{3+}_{0.0191}Vac_{0.0010}O$, where Vac indicates vacancy in the cation site. Since the amounts of ferric iron and vacancies are small, their effects on elasticity are considered negligible [11].

High-pressure experiments were performed using clock-type diamond anvil cells (DACs) [12] with rhenium gaskets. Samples for high-pressure measurements were processed by focused ion beam milling with gallium ions. The processed crystal was placed on the culet of a diamond anvil. The tiny crystal and ruby chips, used as a pressure marker, were sealed into the DAC with compressed helium gas using a gas-loading system at SPring-8. The crystal orientation and crystallinity of the crystal in the DAC was confirmed using an x-ray precession camera or a four-circle diffractometer.

IXS measurements were performed at BL35XU of SPring-8 [13] at 17.747 keV, using a Si (9 9 9) backscattering geometry with ~3 meV energy resolution (full width at half maximum (FWHM)). The samples were mounted on an Eulerian cradle. The incident beam size for the ambient-condition measurement was ca $70 \times 50$ $\mu$m$^2$ (FWHM). For measurements under pressure, a compound focusing system was used to make the incident beam size ca. $17 \times 16$ $\mu$m$^2$ (FWHM) [14]. The lattice constant and the crystal orientation matrix of ferropericlase at each pressure condition were determined by measuring the (1 1 1), (2 0 0), and (2 2 0) Brag reflections. Measurements on high-pressure samples were performed at **q** = (0.5, 0, 0) in reciprocal lattice units for B1 structure to investigate the TA phonon far from the Brillouin zone center. In ambient conditions, phonons very close to the (1 1 1) Bragg spot of B1

**Table 1.** Hubbard $U$ parameters and volumes $V$ for Mg$_3$FeO$_4$ at 0 K.

| Pressure (GPa) | High-spin state | | Low-spin state | |
|---|---|---|---|---|
| | $U$ (eV) | $V$ (a.u.$^3$) | $U$ (eV) | $V$ (a.u.$^3$) |
| 0 | 5.46 | 513.14 | — | — |
| 15 | 5.43 | 481.72 | — | — |
| 30 | 5.45 | 450.17 | 7.23 | 427.97 |
| 60 | 5.53 | 412.86 | 7.98 | 394.42 |

structure were also measured to compare with theoretical results. The energy scans were done only over the Stokes modes and the range was up to 100 (40) meV for ambient (high-pressure) samples. Typical accumulation time for one set of twelve IXS spectra was 5 h.

## 3. Calculations

Phonon properties of iron-bearing magnesium oxide were calculated by the direct method with Hellmann–Feynman forces on the basis of the first-principles internally consistent LDA + $U$ formalism using the Quantum ESPRESSO package [15]. Kinetic energy cutoff for wavefunctions was 70 Ry. Convergence threshold on total energy was $10^{-9}$ Ry. Details of the calculation for Mg$_7$FeO$_8$ ($X_{Fe} = 0.125$) are shown in elsewhere [9]. We also did calculations for Mg$_3$FeO$_4$ ($X_{Fe} = 0.25$). Parameters are shown in table 1. Phonopy [16] was used to determine Born–von Karman force constant matrices and solve the dynamical problem. Supercells were used to accurately determine the phonon dispersion away from the zone center. The number of atoms in a supercell was 128 and 64 for Mg$_7$FeO$_8$ and Mg$_3$FeO$_4$, respectively, corresponding to $2 \times 2 \times 2$ of each unit cell. We evaluated the dielectric tensor and effective charges for Mg$_7$FeO$_8$ and Mg$_3$FO$_4$ in the high-spin state by comparing with the IXS spectrum of ferropericlase in ambient conditions. We also calculated these quantities for MgO using density functional perturbation theory (DFPT).

The results of the calculations were used to simulate IXS spectra. The IXS intensity is proportional to the dynamic structure factor, which can be written (see, e.g. [8]):

$$S(\mathbf{Q}, \omega)$$
$$= N \sum_{\mathbf{q}} \sum_{\substack{j \\ \text{mode}}}^{3r} \left| \sum_{\substack{d \\ \text{Atom/cell}}}^{r} \frac{f_d(\mathbf{Q})}{\sqrt{2M_d}} \mathbf{Q} \cdot \mathbf{e}_{\mathbf{q}jd} \exp\left[-W_d(\mathbf{Q}) + i\mathbf{Q} \cdot \mathbf{x}_d\right] \right|^2 F_{\mathbf{q}j}(\omega),$$

where $N$ is the number of unit cells illuminated by the x-ray beam, $\mathbf{Q}$ is the total momentum transfer, $\mathbf{q}$ is the reduced momentum transfer within the first Brillouin zone or the phonon momentum or propagation direction, $d$ is an index that runs over the $r$ atoms in the primitive cell located at $\mathbf{x}_d$, and $j$ is the phonon mode index that runs over the $3r$ modes expected at any $\mathbf{q}$. $f_d(\mathbf{Q})$ is the atomic form factor. $M_d$ is the atomic mass. $\mathbf{e}_{\mathbf{q}jd}$ is the phonon polarization. The Debye–Waller factor, $\exp[-W_d(\mathbf{Q})]$ was assumed to be atom-independent and treated as a part of the scaling factor in the present calculations.

$F_{\mathbf{q}j}(\omega)$ describes the spectral shape and the temperature dependent intensity of the phonon mode. We adopt the pseudo-Voigt function weighted with the Bose occupation factor and $1/\omega_{\mathbf{q}j}$. The full width at half maximum of the profile function was 3.0 meV, which is the typical energy resolution of the present IXS experiments. The lattice symmetry of ferropericlase was observed to be cubic, whereas the calculations gave a tetragonal structure for ferropericlase with high-spin iron. Therefore, we assumed that an experimental IXS spectrum at $\mathbf{Q} = (H, K, L)$ is average of those at $\mathbf{Q} = (H, K, L)$, $(H, L, K)$, $(K, L, H)$, $(K, H, L)$, $(L, H, K)$, and $(L, K, H)$ from calculations.

## 4. Results and discussion

### 4.1. Comparison between experimental and calculated IXS spectrum in ambient conditions

Experimental IXS spectra of the sample in ambient conditions are shown in figure 1 by blue crosses. Two large and one small peak are observed at $\mathbf{Q} = (1.00, 1.05, 1.00)$ in reciprocal lattice units for B1 structure (figure 1(a)). The phonon momentum, $q$, is 0.75 nm$^{-1}$ at this $\mathbf{Q}$. The peak top energies are 26.2, 47.8, and 87.1 meV. Calculated spectra for MgO are shown together with black lines. The positions of two large peaks agree with those reported in a previous study [17], 48.2 and 88.9 meV at $\mathbf{q} = (0, 0, 0)$. These two modes at can be assigned to the transverse optic (TO) and longitudinal optic (LO) modes [17]. The small peak at 26.2 meV does not appear in MgO at this $\mathbf{Q}$ and is related to vibration of the iron atom judging from partial vibrational density of states for iron [9]. The experimental spectrum shows lower energy for the TO mode than those in the calculated MgO spectrum. In contrast, the almost identical peak positions for MgO (calculation) and ferropericlase (experiment) at 87.1 meV suggest independence of the peak energy of the LO mode from the iron content. The experimental spectrum at $\mathbf{Q} = (2.00, 0.50, 0.00)$, where the phonon momentum is 7.42 nm$^{-1}$, shows a broad transverse phonon band at 16–33 meV, whereas the calculated MgO spectrum gives a relatively sharp peak at 27.1 meV (figure 1(b)). The position of the calculated MgO peak agrees to the TA mode energy in the previous study [17], 26.2 meV at $\mathbf{q} = (0, 0, 0.5)$. From these comparisons between MgO and ferropericlase, the iron substitution decreases the phonon energy in the lower energy region and has less impact at higher energy.

We estimated effective charges $Z^*$ and a high-frequency dielectric tensor $\varepsilon_\infty$ by comparing the calculations to the experimental spectrum. A simulated IXS spectrum of Mg$_{1-x}$Fe$_x$O obtained by the direct method does not show LO-TO spitting without taking long-range interactions into account. Since the LO-mode energy of ferropericlase was almost identical to that of MgO (figure 1(a)), we take the energy of the LO mode to be independent of iron content in this study. We optimized the non-analytical parameters in two ways: (1) Seek $Z^*$ with a fixed $\varepsilon_\infty$ or (2) Seek $\varepsilon_\infty$ with fixed $Z^*$. Here, it was assumed the off-diagonal elements of $\varepsilon_\infty$ and $Z^*$ were zero. From a DFPT calculation, the values of $\varepsilon_\infty$ and $|Z^*|$ were calculated for MgO to be 3.09 and 1.93, respectively. Those for FeO were estimated from inelastic neutron scattering measurements to
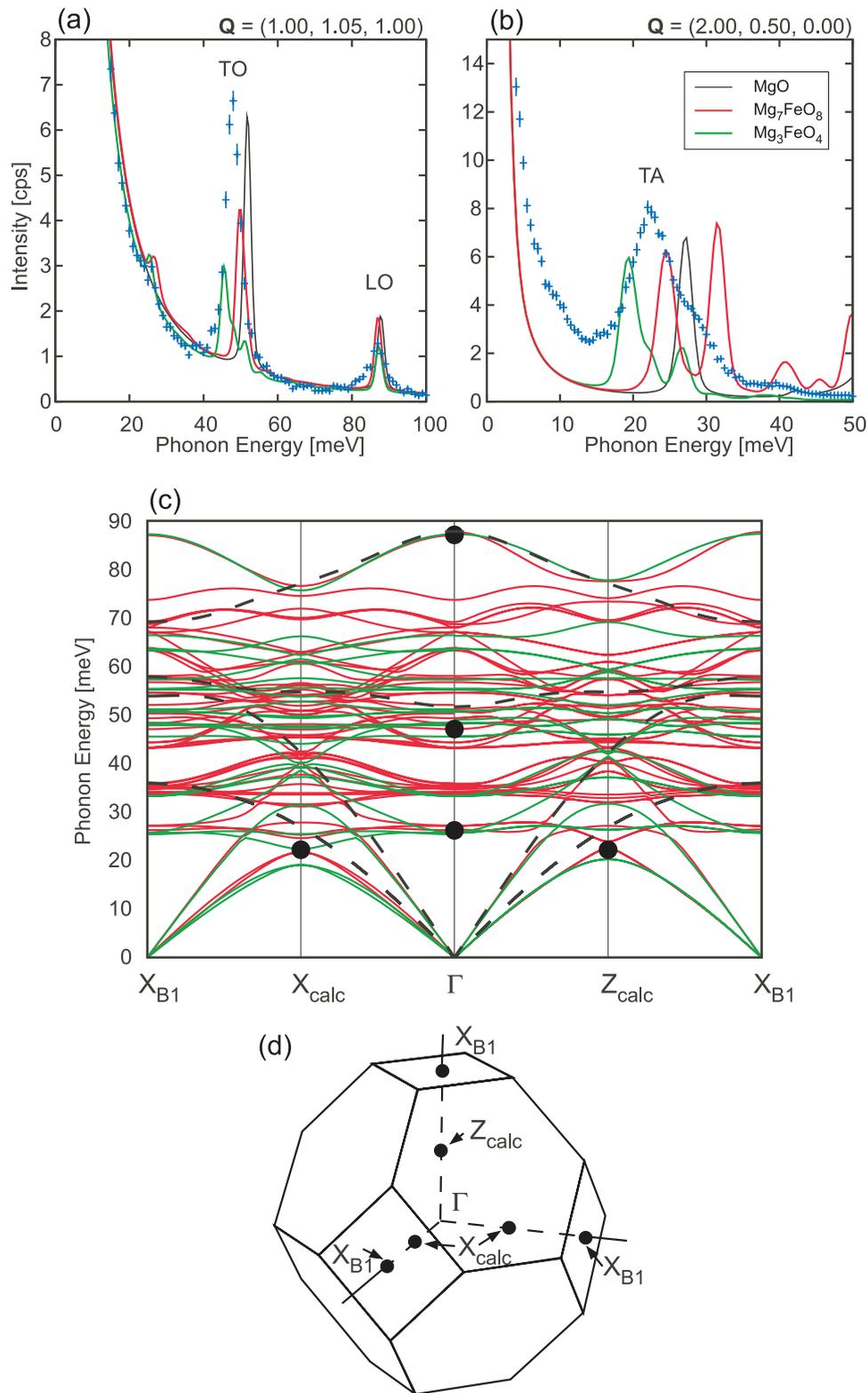
**Figure 1.** Results in ambient conditions. Experimental and calculated IXS spectra at **Q** = (1.00, 1.05, 1.00) (a) and at **Q** = (2.00, 0.50, 0.00) (b) in reciprocal lattice units of B1 structure in ambient conditions (0 GPa). Blue crosses indicate the experimental spectra. Thin black curves indicate calculated spectra of MgO by DFPT. Thick curves are calculated spectra of $Mg_7FeO_8$ (red) and $Mg_3FeO_4$ (green) using the direct method with the non-analytic correction. An elastic component was added to each calculated spectrum. Iron was treated in high spin state. (c) Calculated dispersion curves for $Mg_7FeO_8$ (red), $Mg_3FeO_4$ (green), and MgO (black broken). The peak positions in the experimental spectra are shown by black circles. Because superlattices were used for calculation, the special points on the Brillouin zone boundary ($X_{calc}$ and $Z_{calc}$) are located in the Brillouin zone for B1 structure. (d) The first Brillouin zone of a face centered lattice (B1 structure). The special points for B1 structure ($X_{B1}$) and the superlattice used for the calculations ($X_{calc}$ and $Z_{calc}$) are shown by black circles.

**Table 2.** Non-analytical parameters of $Mg_{1-x}Fe_xO$ with high spin iron. (Case 1) Effective charges are optimized with fixed dielectric constants. (Case 2) Dialectic constants are optimized with fixed effective charges.

| X | Case 1 | | Case 2 | |
|---|---|---|---|---|
| | $\frac{1}{3}Tr(\varepsilon_\infty)$ (fix) | $\frac{1}{3}|Tr(Z^*)|$ | $\frac{1}{3}Tr(\varepsilon_\infty)$ | $\frac{1}{3}|Tr(Z^*)|$ (fix) |
| 0.125 | 3.86 | 2.19 | 3.02 | 1.94 |
| 0.25 | 4.63 | 2.52 | 2.78 | 1.95 |

be 9.24 and 2.00, respectively [18]. In the first method, we took the three diagonal elements of $\varepsilon_\infty$ to be 3.86 and 4.63 for $X_{Fe} = 0.125$ and 0.25, respectively, from linear interpolation between these values. In the second method, we assumed the $|Z^*|$ for all atoms to be 1.94 or 1.95, also from the linear interpolation. The non-analytic parameters were determined to reproduce the experimental LO-mode energy. We assumed, for simplicity, that the all atoms have the same $|Z^*|$. The optimized non-analytic parameters are shown in table 2. The real $|Z^*|$ and $\varepsilon_\infty$ are probably between these values. These values are not located between those of MgO and FeO.

IXS spectra for $Mg_{1-x}Fe_xO$ in the high-spin state were calculated taking the long range electric field effect into account. Calculated phonon dispersion curves along $\Gamma$-$X_{B1}$ in the first Brillouin zone of a face centered lattice (B1 structure of MgO: figure 1(d)) are shown in figure 1(c). The subscript B1 indicate that these special points are for B1 structure. Note that calculated energies for acoustic phonons are zero at the $X_{B1}$ points because we used the supercells for the calculation. Special points on the Brillouin zone boundary for the supercells are shown in figure 1 by $X_{calc}$ and $Z_{calc}$, which correspond to **q** of (0.5, 0, 0) and (0, 0, 0.5) in reciprocal lattice units of B1 structure, respectively. The experimental high-intensity peak position is located between those calculated for $Mg_7FeO_8$ (red) and $Mg_3FeO_4$ (green). This indicates that the energy of the main phonon peaks decreases by the cation substitution. The calculated spectrum of $Mg_3FeO_4$ near the $\Gamma$ point (figure 1(a)) shows a strong peak at 47 meV and small peaks at the high-energy side. Around this energy, the experiment shows a single peak, which is similar to that of $Mg_7FeO_8$. In contrast, the phonon band in the experimental spectrum far from the Brillouin zone center is in better agreement with $Mg_3FeO_4$ than $Mg_7FeO_8$ (see around 15–35 meV range in figure 1(b)). From these comparisons, IXS spectra about the TA mode of the present sample are interpreted based on calculated ones for $Mg_3FeO_4$.

### 4.2. Transverse phonon under pressure

The lattice constant and the crystal orientation matrix of ferropericlase were refined at each pressure before measuring transverse phonon with **q** = (0.5, 0, 0). Three Bragg spots (1 1 1), (2 0 0), and (0 2 2) were used for this purpose. The rocking curve widths of these Bragg reflections were less than 0.4 degrees in FWHM even at the highest pressure condition. The unit cell volumes were plotted in figure 2 together with
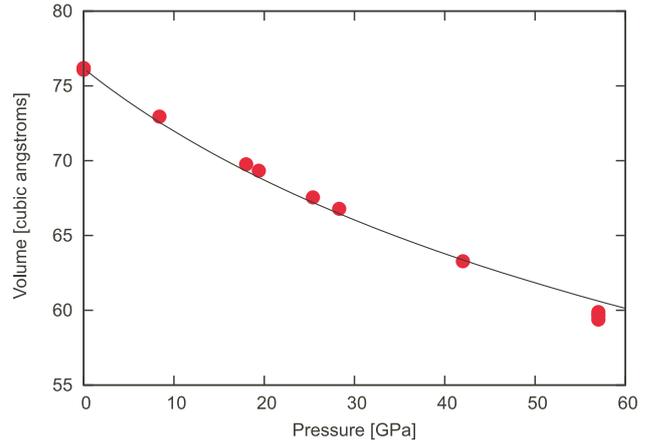


**Figure 2.** Pressure variation of the volume of $4Mg_{1-x}Fe_xO$. Symbols was obtained from three Bragg spots measured before and after IXS measurement at each pressure condition. Error bars are smaller than symbols. The line is a reported compression curve for high spin state with $x = 0.20$ [19].

a reported equation of state (EoS) for high spin state with $X_{Fe} = 0.20$ [19]. The present volumes are slightly larger than those from the EoS below 30 GPa and slightly smaller above that pressure, indicating the spin transition occurred at 30 GPa. This is reasonable considering the sensitivity of the transition pressure to the iron content [19].

Figure 3(a) shows experimental IXS spectra for ferropericlase at **q** = (0.5, 0, 0). A pseudo-Voigt function was fitted to this TA phonon band. The pressure variation of the phonon energy was plotted in figure 3(b). The energy of the phonon increases with increasing pressure up to 10 GPa, is relatively flat from 10 to 30 GPa, and then increased again above this pressure where the spin transition occurred (see dashed lines in figure 3(b)).

Simulated IXS spectra of $Mg_3FeO_4$ at high-pressure conditions were compared with the experimental ones since they show better agreement far from the Brillouin zone center (figure 1(b)). We calculated IXS spectra of ferropericlase in the high-spin state at 0, 15, 30, and 60 GPa and in the low-spin state at 30 and 60 GPa. The long range electric field effect was ignored since this effect does not appear far from the Brillouin zone center. Peak positions were evaluated by fitting a pseudo-Voigt function with $\eta = 0.5$ to the calculated spectra between 15 and 25 meV. The calculated results show that the TA phonon energy of high-spin ferropericlase only weakly increases from 0 to 30 GPa and does not change to 60 GPa (red circles in figure 3(c)). For low-spin ferropericlase, the TA phonon energy is not so different between 30 and 60 GPa though slightly increasing (green circles in figure 3(c)). It is reported that MgO also shows weak pressure dependence of the TA-mode energy along [1 0 0] direction of B1 structure [20]. The energy of TA phonon along the [1 0 0] direction does not change with pressure as long as the electronic state is essentially unchanged.

Based on the results from the present calculations (figure 3(c)), we conclude that the observed rapid increase of the TA phonon energy above 30 GPa (figure 3(b)) is due to the spin transition. As found in the calculations, the TA energy
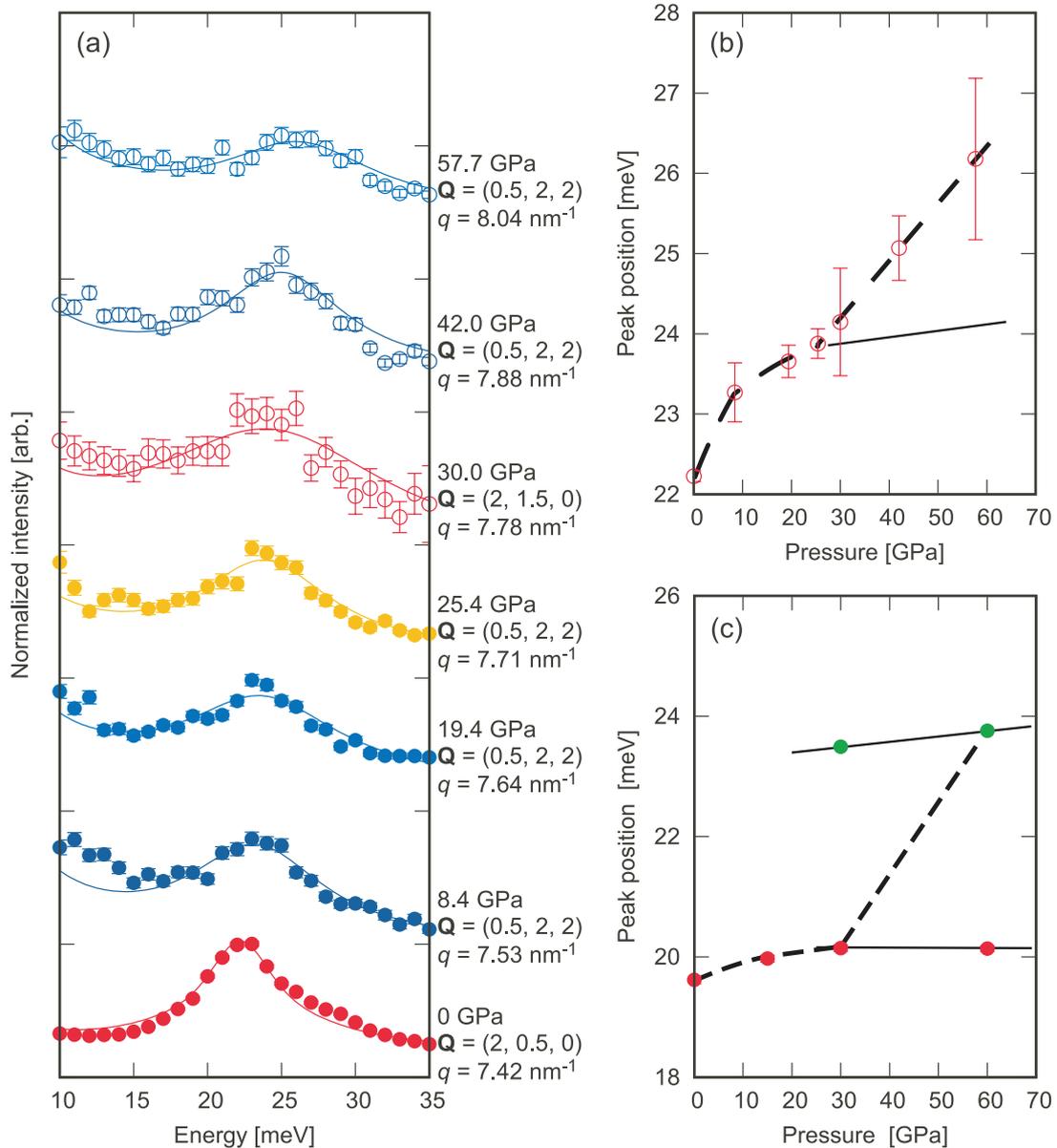
**Figure 3.** TA phonon mode of ferropericlase. (a) Experimental IXS spectra of **q** = (0.5, 0.0, 0.0) at various pressure conditions. Total momentum transfers, **Q**, are shown next to spectra. The phonon momenta, $q$, are also shown in nm$^{-1}$ unit. Lines are two pseudo-Voigt functions (one is for elastic line and the other is for TA phonon peak) fitted to spectra. The spectra were normalized at the TA phonon peak and offset for easy comparison. (b) Pressure variation of TA phonon energy at **q** = (0.5, 0.0, 0.0) obtained from spectra shown in figure 3(a). Vertical bars indicate fitting errors of the energy. Solid and dashed lines are just guides for eyes. A dotted line is a linear line between the data points at 8.4 and 57.7 GPa. (c) Pressure variation of TA phonon energy from a calculated spectrum at each pressure and spin state fitting to a pseudo-Voigt function with $\eta = 0.5$. Red and green circles are for high-spin and low-spin, respectively. Solid and dashed lines are guides for eyes.

of ferropericlase in the high- and low-spin states shows weak pressure dependence. The calculations revealed that the TA energy is higher in the low-spin state than in the high-spin state. At the spin-transition pressure, the TA energy was observed to increase rapidly with pressure. The phonon hardens across the spin transition.

We calculated phonon dispersion relationship of ferropericlase in the high- and low-spin states as shown in figure 4 to understand why the TA phonon energy of the low-spin ferropericlase is higher than that of the high-spin one. In high-spin ferropericlase, there are large gaps in phonon energy at $X_{calc}$ and $Z_{calc}$, corresponding to **q** = (0.5, 0, 0) in the experiments.

This gap is between the TA mode and the lowest-energy-optic mode. In contrast, the gap is almost closed in low-spin ferropericlase.

To try to understand the microscopic basis for the calculated hardening, we investigated calculated interatomic force constant matrices to find out how different they are between the high and low spin states. The results show that the absolute values of the transverse elements between iron and the nearest neighbor oxygen are much larger in the low spin state than in the high spin state. Those values between iron and that in the next unit cell are also larger. In contrast, the change in the absolute values of the longitudinal elements between the high- and
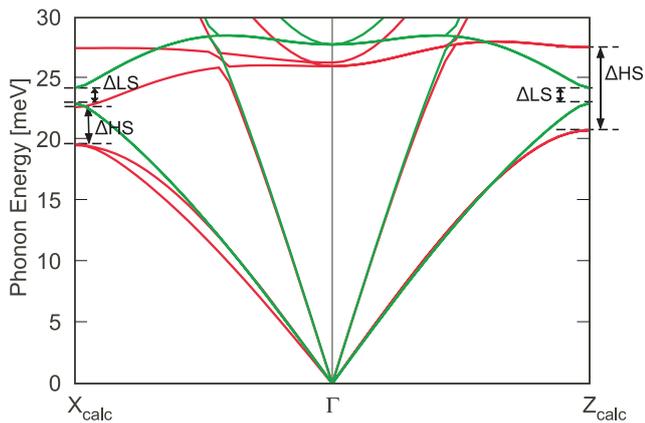
**Figure 4.** Low energy part of calculated dispersion curves for Mg$_3$FeO$_4$ at 30 GPa in the high-spin state (red) and in the low-spin state (green). $X_{calc}$ and $Z_{calc}$ indicate special points on the Brillouin zone boundary of the feropericlase structure for the calculation, corresponding to **q** of (0.5, 0, 0) and (0, 0, 0.5) for B1 structure, respectively (see figure 1). The phonon gaps between the TA and the lowest-energy-optic modes at 30 GPa are shown by $\Delta$HS and $\Delta$LS for the high- and low-spin states, respectively. The gap in the high-spin state is widely open, whereas that in the low-spin state is almost closed.

low-spin states is less and that in force constants related to magnesium is negligibly small. The large increase in the transvers elements related to iron atoms in the interatomic force constant matrices most probably causes the phonon gap closing in the low spin state. This is consistent with discussion on a phonon gap at the zone boundary in a diatomic linear chain model [21].

The present finding can explain discrepancy between previous studies. The TA phonon energy does not increase with pressure in high-spin feropericlase above 15 GPa and then increase through the spin transition. It seems as if the TA phonon energy far from the Brillouin zone center is softened by compression (figures 3 and 4). The TA phonon anomaly observed by IXS at lower **q** then may originate at higher **q**; this anomaly is therefore observed by IXS clearly [4] and not by the light scattering [6].

## 5. Conclusion

We have performed IXS measurements on the phonons of Mg$_{0.8310}$Fe$_{0.1594}$O feropericlase. The TA phonon energy was found to increase suddenly above the spin-transition pressure. Consequently, the TA phonon energy around the spin-transition pressure seems anomalous. Simulated IXS spectra of Mg$_3$FeO$_4$ with high- and low-spin state iron based on the first principles calculations displayed that the energy of the TA phonon far from the Brillouin zone center is higher in the low-spin state than in the high-spin state; and that the phonon gap between the TA and the lowest-energy-optic modes is much narrower in the low-spin state than in the high-spin state. The calculations also revealed that these TA phonon energies for high- and low-spin state does not change so much with compression. On the basis of the present results, we have concluded that the phonon gap narrowing at $X_{calc}$ and $Z_{calc}$, or **q** = (0.5, 0, 0) for B1 structure, through the spin transition is

related with the observed TA phonon anomaly and explains the contradictory results in the previous experimental studies.

## References

[1] Badro J, Fiquet G, Guyot F, Rueff J P, Struzhkin V V, Vankó G and Monaco G 2003 *Science* **300** 789
[2] Crowhurst J C, Brown J M, Goncharov A F and Jacobsen S D 2008 *Science* **319** 451
[3] Marquardt H, Speziale S, Reichmann H J, Frost D J, Schilling F R and Garnero E J 2009 *Science* **324** 224
[4] Antonangeli D, Siebert J, Aracne C M, Farber D L, Bosak A, Hoesch M, Krisch M, Ryerson F J, Fiquet G and Badro J 2011 *Science* **331** 64
[5] Murakami M, Ohishi Y, Hirao N and Hirose K 2012 *Nature* **485** 90
[6] Yang J, Tong X, Lin J F, Okuchi T and Tomioka N 2015 *Sci. Rep.* **5** 17188
[7] Crowhurst J C, Abramson E H, Slutsky L J, Brown J M, Zaug J M and Harrell M D 2001 *Phys. Rev.* B **64** 100103
[8] Baron A Q R 2016 *Synchrotron Light Sources and Free-Electron Lasers* (New York: Springer) p 1721
[9] Fukui H, Tsuchiya T and Baron A Q R 2012 *J. Geophys. Res.* **117** B12202
[10] Wu Z, Justo J F and Wentzcovitch R M 2013 *Phys. Rev. Lett.* **110** 228501
[11] Jacobsen S D, Reichmann H J, Spetzler H A, Mackwell S J, Smyth J R, Angel R J and McCammon C A 2002 *J. Geophys. Res.* **107** 2037
[12] Yamaoka S, Fukunaga O, Shimomura O and Nakazawa H 1979 *Rev. Sci. Instrum.* **50** 1163
[13] Baron A Q R, Tanaka Y, Goto S, Takeshita K, Matsushita T and Ishikawa T 2000 *J. Phys. Chem. Solids* **61** 461
[14] Ishikawa D, Uchiyama H, Tsutsui S, Fukui H and Baron A Q R 2013 *Proc. SPIE* **8848** 88480F
[15] Giannozzi P *et al* 2009 *J. Phys.: Condens. Matter* **21** 395502
[16] Togo A, Oba F and Tanaka I 2008 *Phys. Rev.* B **78** 134106
[17] Sangster M J L, Peckham G and Saunderson D H 1970 *J. Phys.* C **3** 1026
[18] Kugel G, Carabatos C, Hennion B, Prevot B, Revcolevschi A and Tocchetti D 1977 *Phys. Rev.* B **16** 378
[19] Fei Y, Zhang L, Corgne A, Watson H, Ricolleau A, Meng Y and Prakapenka V 2007 *Geophys. Res. Lett.* **34** L17307
[20] Karki B B, Wentzcovitch R M, de Gironcoli S and Baroni S 2000 *Phys. Rev.* B **61** 8793
[21] Ashcroft A N and Mermin N D 1976 *Solid State Physics* (Philadelphia: Saunders College Publishing) ch 22